Exact Solutions of Electromagnetic Fields in Both Near and Far Zones Radiated by Thin Circular-Loop Antennas: A General Representation

Le-Wei Li, *Senior Member, IEEE*, Mook-Seng Leong, *Member, IEEE*, Pang-Shyan Kooi, *Member, IEEE*, and Tat-Soon Yeo, *Senior Member, IEEE*

***Abstract*— This paper presents an alternative vector analysis of the electromagnetic (EM) fields radiated from thin circular-loop antennas of arbitrary radius a. This method, which employs the dyadic Green's function in the derivation of the EM radiated fields, makes the analysis more general, compact, and straightforward than those two methods published recently by Werner and Overfelt. Both near and far zones are considered so that the EM radiated fields are expressed in terms of the vector-wave eigenfunctions. Not only the exact solution of the EM fields in the near and far zones outside the region (where $r > a$) is derived by the use of the spherical Hankel function of the first kind, but also the closed-series form of the EM fields radiated in the near zone inside the region $0 \leq r < a$ is obtained in series of the spherical Bessel functions of the first kind. As an example, a Fourier cosine series is used to expand an arbitrary current distribution along the loop and the exact representations of the EM radiated fields due to the loop everywhere are obtained in closed form. The closed form reduces to those for the sinusoidal current loop and further for the uniform current loop. Validity of the approximate formulas is discussed and clarified. Error analysis based on numerical computations of the radiated fields is also given to show the accuracy of the limiting cases.**

***Index Terms*— Closed-form solution, eigenfunction expansion, electromagnetic radiation, loop antennas, vector-wave functions.**

I. Introduction

THIN circular-loop antennas carrying different forms of the currents and their radiation characteristics have been investigated by many researchers over the last several decades. Literature is readily available for the circular loops located in free-space [3]–[12] and immersed in layered media [13]–[15]. The radiation characteristics of the circular-loop antennas can also be readily found from antenna textbooks [16]–[22].

As stated and reviewed in [1] and [2], many papers dealt with the radiated fields in the far zone due to circular loops with certain restrictions, e.g., the far field due to a uniform current [3], the distant-field due to a sinusoidal current [4], the approximate and exact far-zone field due to a hyperbolic cosine current distribution of a small loop [5] and a larger loop [6], and the far-field intensities due to a Fourier cosine series current [10] and a traveling-wave current distribution [11].

Manuscript received May 21, 1996. This work was supported by research Grant RP950646 from the National University of Singapore.

The authors are with the Communications & Microwave Division, Department of Electrical Engineering, National University of Singapore, 119260 Singapore.

Publisher Item Identifier S 0018-926X(97)08805-4.

For the near-zone field, only a small amount of work [9] has been reported in the literature due to the difficulty in evaluating integrals analytically. Recently, Werner [1] employed the Lommel expansion and the Euler's identity to evaluate the Hertzian potential integral and further express the electromagnetic components in terms of the spherical Bessel functions and the spherical harmonics. An arbitrary current is assumed [9] at the beginning; but later a Fourier series is employed to obtain general results in closed form and, finally, a cosine current distribution and, further, a constant current density are considered to specify the obtained general results. In the meantime, Overfelt [2] assumed a constant current distribution of the thin loop antenna and derived the series form of Hertzian potential and, thereafter, the radiated near-zone field by means of elliptic integrals. The two papers contribute significantly to the exact evaluation of the electromagnetic radiated fields in the near zone.

However, the results obtained [1], [2] are, as indicated by Overfelt, valid only for the region $r < a$ where a is the radius of the loop. Also, the techniques presented in the two papers is not so straightforward and general. This paper aims at providing a more general, straightforward and simple method to obtain the electromagnetic radiated fields in closed form. Both the exact near fields without the restriction on the observation point r (i.e., valid for both $0 \leq r < a$ and $r > a$) and the exact far field are obtained regardless of the dimensions of the loop antennas. Also, the improper statement of the validity of the approximate formulas to be deduced is pointed out.

II. General Formulation of Electromagnetic Radiated Fields

Consider the geometry in Fig. 1 where the origin of the spherical coordinates is located at the center of a thin circular-loop antenna.

Similar to [1, Eq. (22)], the volumetric electric current density may be expressed as

$$\boldsymbol{J}(\boldsymbol{r}') = \frac{I(\phi')\delta(r'-a)\delta\left(\theta' - \dfrac{\pi}{2}\right)}{a}\hat{\boldsymbol{\phi}} \tag{1}$$

where $I(\phi')$ is an arbitrary function of ϕ', and a is the radius of the circular loop. This current distribution radiates the

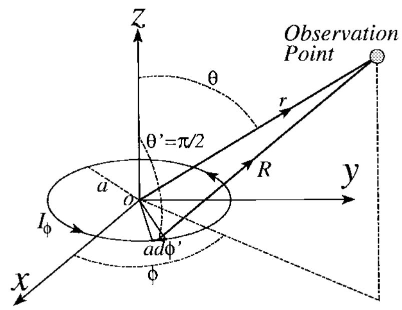

Fig. 1. Geometry of a thin circular-loop antenna.

electromagnetic waves into the free-space. The equations for determining the electromagnetic radiated fields are given as follows [23], [24]:

$$\boldsymbol{E} = i\omega\mu_0 \iiint_V \overline{\boldsymbol{G}}_{EJ0}(\boldsymbol{r},\boldsymbol{r}') \cdot \boldsymbol{J}(\boldsymbol{r}')\, dV' \tag{2a}$$

$$\boldsymbol{H} = \iiint_V \nabla \times \overline{\boldsymbol{G}}_{EJ0}(\boldsymbol{r},\boldsymbol{r}') \cdot \boldsymbol{J}(\boldsymbol{r}')\, dV' \tag{2b}$$

where the subscript V represents the volume occupied by the circular loop and $\overline{\boldsymbol{G}}_{EJ0}(\boldsymbol{r},\boldsymbol{r}')$ denotes the dyadic Green's function of the electric kind in free-space.

The dyadic Green's function of the electric kind in free-space was given earlier in terms of the spherical vector-wave functions by Tai [23] and applied by Li *et al.* [24] recently. The magnetic kind can be obtained by simply applying the duality relations to the electric kind. It is found that the forms of the dyadic Green's functions of electric and magnetic kinds are of the same form and given by

$$\overline{\boldsymbol{G}}_{EJ0}(\boldsymbol{r},\boldsymbol{r}') = -\frac{\hat{\boldsymbol{r}}\hat{\boldsymbol{r}}}{k_0^2}\delta(\boldsymbol{r}-\boldsymbol{r}') + \frac{ik_0}{4\pi}\sum_{n=1}^{\infty}\sum_{m=0}^{n}(2-\delta_{m0})D_{mn} \cdot \begin{cases} \boldsymbol{M}^{(1)}_{{}^e_o mn}\boldsymbol{M}'_{{}^e_o mn}(k_0) + \boldsymbol{N}^{(1)}_{{}^e_o mn}(k_0)\boldsymbol{N}'_{{}^e_o mn}(k_0) \\ \qquad r \geq r' \\ \boldsymbol{M}_{{}^e_o mn}(k_0)\boldsymbol{M}'^{(1)}_{{}^e_o mn}(k_0) + \boldsymbol{N}_{{}^e_o mn}(k_0)\boldsymbol{N}'^{(1)}_{{}^e_o mn}(k_0) \\ \qquad r \leq r' \end{cases} \tag{3}$$

where δ_{mn} ($= 1$ for $m = n$; and 0 for $m \neq n$) denotes the Kronecker symbol, and the normalization coefficient D_{mm} is given by

$$D_{mn} = \frac{(2n+1)}{n(n+1)}\,\frac{(n-m)!}{(n+m)!}.$$

In (3), the vector-wave eigenfunctions are defined in the spherical coordinates system as follows:

$$\begin{aligned}\boldsymbol{M}_{{}^e_o mn}(k) = &\mp \frac{mz_n(kr)}{\sin\theta}P_n^m(\cos\theta)\begin{matrix}\sin\\ \cos\end{matrix} m\phi\hat{\boldsymbol{\theta}} \\ &- z_n(kr)\frac{dP_n^m(\cos\theta)}{d\theta}\begin{matrix}\cos\\ \sin\end{matrix} m\phi\hat{\boldsymbol{\phi}}\end{aligned} \tag{4a}$$

$$\begin{aligned}\boldsymbol{N}_{{}^e_o mn}(k) = &\frac{n(n+1)z_n(kr)}{kr}P_n^m(\cos\theta)\begin{matrix}\cos\\ \sin\end{matrix} m\phi\hat{\boldsymbol{r}} \\ &+ \frac{\partial[rz_n(kr)]}{kr\partial r}\,\frac{dP_n^m(\cos\theta)}{d\theta}\begin{matrix}\cos\\ \sin\end{matrix} m\phi\hat{\boldsymbol{\theta}} \\ &\mp \frac{m}{\sin\theta}\,\frac{\partial[rz_n(kr)]}{kr\partial r}P_n^m(\cos\theta)\begin{matrix}\sin\\ cos\end{matrix} m\phi\hat{\boldsymbol{\phi}}\end{aligned} \tag{4b}$$

where $z_n(k_0r)$, which takes the forms of the spherical Hankel function of the first kind $h_n^{(1)}(k_0r)$ for the fields in the region $r > a$ and the spherical Bessel function of the first kind $j_n(k_0r)$ for the region $0 \leq r < a$, represents the spherical Bessel functions of order n, and $P_n^m(\cos\theta)$ is the associated Legendre function. The notations ${}^e_o mn$ and ${}^o_e mn$ of the dyadic Green's function in (3) mean that the summation form of both even and odd modes should be taken into account when the integral in (2) is evaluated.

Substituting the current distribution in (1) into the integral (2), we have the following general formula for the electromagnetic radiated fields in the region $r \gtrless a$:

$$\begin{aligned}\begin{bmatrix}\boldsymbol{E}^>\\ \boldsymbol{E}^<\end{bmatrix} = -\frac{\eta_0k_0^2}{4\pi}\sum_{n=1}^{\infty}\sum_{m=0}^{n}D_{mn}\Bigg\{&\begin{bmatrix}\boldsymbol{\Phi}^{M<}_{{}^e_o mn}\boldsymbol{M}^{(1)}_{{}^e_o mn}(k_0)\\ \boldsymbol{\Phi}^{M>}_{{}^e_o mn}\boldsymbol{M}_{{}^e_o mn}(k_0)\end{bmatrix} \\ &+ \begin{bmatrix}\boldsymbol{\Phi}^{N<}_{{}^e_o mn}\boldsymbol{N}^{(1)}_{{}^e_o mn}(k_0)\\ \boldsymbol{\Phi}^{N>}_{{}^e_o mn}\boldsymbol{N}_{{}^e_o mn}(k_0)\end{bmatrix}\Bigg\}\end{aligned} \tag{5a}$$

$$\begin{aligned}\begin{bmatrix}\boldsymbol{H}^>\\ \boldsymbol{H}^<\end{bmatrix} = \frac{ik_0^2}{4\pi}\sum_{n=1}^{\infty}\sum_{m=0}^{n}D_{mn}\Bigg\{&\begin{bmatrix}\boldsymbol{\Phi}^{M<}_{{}^e_o mn}\boldsymbol{N}^{(1)}_{{}^e_o mn}(k_0)\\ \boldsymbol{\Phi}^{M>}_{{}^e_o mn}\boldsymbol{N}_{{}^e_o mn}(k_0)\end{bmatrix} \\ &+ \begin{bmatrix}\boldsymbol{\Phi}^{N<}_{{}^e_o mn}\boldsymbol{M}^{(1)}_{{}^e_o mn}(k_0)\\ \boldsymbol{\Phi}^{N>}_{{}^e_o mn}\boldsymbol{M}_{{}^e_o mn}(k_0)\end{bmatrix}\Bigg\}\end{aligned} \tag{5b}$$

where $\eta_0 = 120\pi\Omega$ denotes the intrinsic impedance. The spherical Bessel function of the first kind (i.e., $z_n(k_0r) = j_n(k_0r)$) is used in the vector-wave functions $\boldsymbol{M}_{{}^e_o mn}$ and $\boldsymbol{N}_{{}^e_o mn}$; the spherical Hankel function of the first kind [i.e., $z_n(k_0r) = h_n^{(1)}(k_0r)$ is used in the vector-wave functions $\boldsymbol{M}^{(1)}_{{}^e_o mn}(k_0)$ and $\boldsymbol{M}^{(1)}_{{}^e_o mn}(k_0)$]. They are also used under the same rule in the coefficients of the series EM fields, i.e., $\boldsymbol{\Phi}^{M>}_{{}^e_o mn}$ and $\boldsymbol{\Phi}^{N>}_{{}^e_o mn}$, $\boldsymbol{\Phi}^{M<}_{{}^e_o mn}$ and $\boldsymbol{\Phi}^{N<}_{{}^e_o mn}$. These coefficients are expressed by

$$\begin{aligned}\begin{bmatrix}\boldsymbol{\Phi}^{M<}_{{}^e_o mn}\\ \boldsymbol{\Phi}^{M>}_{{}^e_o mn}\end{bmatrix} &= -a\begin{bmatrix}j_n(k_0a)\\ h_n^{(1)}(k_0a)\end{bmatrix}\frac{dP_n^m(0)}{d\theta} \\ &\cdot \int_0^{2\pi}\begin{matrix}\cos\\ \sin\end{matrix}(m\phi')I(\pi')\,d\phi'\end{aligned} \tag{6a}$$

$$\begin{aligned}\begin{bmatrix}\boldsymbol{\Phi}^{N<}_{{}^e_o mn}\\ \boldsymbol{\Phi}^{N>}_{{}^e_o mn}\end{bmatrix} &= \mp a\begin{bmatrix}\dfrac{d[aj)n(k_0a)]}{k_0ada}\\ \dfrac{d[ah_n^{(1)}(k_0a)]}{da}\end{bmatrix}mP_n^m(0) \\ &\cdot \int_0^{2\pi}\begin{matrix}\sin\\ \cos\end{matrix}(m\phi')I(\phi')\,d\phi'\end{aligned} \tag{6b}$$

and the associated Legendre function $P_n^m(0)$, and its first-order derivative $dP_n^m(0)/d\theta$ are given by

$$\frac{dP_n^m(0)}{d\theta} = -\frac{2^{m+1}\sin\left[\dfrac{1}{2}(n+m)\pi\right]\Gamma\left(\dfrac{n+m}{2}+1\right)}{\sqrt{\pi}\,\Gamma\left(\dfrac{n-m+1}{2}\right)} \tag{7a}$$

$$P_n^m(0) = \frac{2^m\cos\left[\dfrac{1}{2}(n+m)\pi\right]\Gamma\left(\dfrac{n+m+1}{2}\right)}{\sqrt{\pi}\,\Gamma\left(\dfrac{n-m}{2}+1\right)}. \tag{7b}$$

In the above consideration, we did not include the observation points exactly on the spherical surface of the loop radius. In fact, the fields on the surface $r = a$, except where $\theta = \pi/2$, can be expressed by either $\boldsymbol{E}^{>}$ and $\boldsymbol{H}^{>}$ or $\boldsymbol{E}^{<}$ and $\boldsymbol{H}^{<}$ where r is assumed to be a. At the points where $r = a$ and $\theta = \pi/2$, the fields consist of the aforementioned principal-value contribution and the additional contribution due to the singularity term of the dyadic Green's function [i.e., the first term of (3)]. This additional contribution can be easily integrated and analytically obtained, but will not be calculated since it is not practically needed here.

It can be seen from (5) that: 1) the expressions in (5) are the general form of the radiated fields valid for any current distribution; 2) once the current density is specified, the intermediates (6) and therefore the fields in (5) can be obtained in a closed form; 3) the field expressions obtained in (5) are valid for any observation point, i.e., for both the regions where $r > a$ and $0 \leq r < a$; and 4) the fields in (5) are given in compact vector form, which can reduce to the scalar form, e.g.,

$$\begin{bmatrix} E_r^{>} \\ E_r^{<} \end{bmatrix} = -\frac{\eta_0 k_0^2}{4\pi}\sum_{n=1}^{\infty}\sum_{m=0}^{n} D_{mn}\begin{bmatrix} \boldsymbol{\Phi}^{N<}_{\substack{e\\o}mn}\dfrac{n(n+1)h_n^{(1)}(k_0r)}{k_0r} \\ \boldsymbol{\Phi}^{N>}_{\substack{e\\o}mn}\dfrac{n(n+1)j_n(k_0r)}{k_0r}\end{bmatrix} \cdot P_n^m(\cos\theta)\begin{matrix}\cos\\ \sin\end{matrix}(m\phi) \tag{8a}$$

$$\begin{bmatrix} E_\theta^{>} \\ E_\theta^{<} \end{bmatrix} = -\frac{\eta_0 k_0^2}{4\pi}\sum_{n=1}^{\infty}\sum_{m=0}^{n} D_{mn}\left\{ \mp\begin{bmatrix} \boldsymbol{\Phi}^{M<}_{\substack{e\\o}mn}h_n^{(1)}(k_0r) \\ \boldsymbol{\Phi}^{M>}_{\substack{e\\o}mn}j_n(k_0r)\end{bmatrix} \cdot \frac{m}{\sin\theta}P_n^m(\cos\theta)\begin{matrix}\sin\\ \cos\end{matrix}(m\phi) + \frac{dP_n^m(\cos\theta)}{d\theta} \cdot \begin{matrix}\cos\\ \sin\end{matrix}(m\phi)\begin{bmatrix} \boldsymbol{\Phi}^{N<}_{\substack{e\\o}mn}\dfrac{d[rh_n^{(1)}(k_0r)]}{k_0rdr} \\ \boldsymbol{\Phi}^{N>}_{\substack{e\\o}mn}\dfrac{d[rj_n(k_0r)]}{k_0rdr}\end{bmatrix}\right\} \tag{8b}$$

$$\begin{bmatrix} E_\phi^{>} \\ E_\phi^{<} \end{bmatrix} = -\frac{\eta_0 k_0^2}{4\pi}\sum_{n=1}^{\infty}\sum_{m=0}^{n} D_{mn}\left\{ -\begin{bmatrix} \boldsymbol{\Phi}^{M<}_{\substack{e\\o}mn}h_n^{(1)}(k_0r) \\ \boldsymbol{\Phi}^{M>}_{\substack{e\\o}mn}j_n(k_0r)\end{bmatrix} \cdot \frac{dP_n^m(\cos\theta)}{d\theta}\begin{matrix}\cos\\ \sin\end{matrix}(m\phi) \mp \frac{m}{\sin\theta}P_n^m(\cos\theta) \cdot \begin{matrix}\sin\\ \cos\end{matrix}(m\phi)\begin{bmatrix} \boldsymbol{\Phi}^{N<}_{\substack{e\\o}mn}\dfrac{d[rh_n^{(1)}(k_0r)]}{k_0rdr} \\ \boldsymbol{\Phi}^{N>}_{\substack{e\\o}mn}\dfrac{d[rj_n(k_0r)]}{k_0rdr}\end{bmatrix}\right\} \tag{8c}$$

and

$$\begin{bmatrix} H_r^{>} \\ H_r^{<} \end{bmatrix} = \frac{ik_0^2}{4\pi}\sum_{n=1}^{\infty}\sum_{m=0}^{n} D_{mn}\begin{bmatrix} \boldsymbol{\Phi}^{M<}_{\substack{e\\o}mn}\dfrac{n(n+1)h_n^{(1)}(k_0r)}{k_0r} \\ \boldsymbol{\Phi}^{M>}_{\substack{e\\o}mn}\dfrac{n(n+1)j_n(k_0r)}{k_0r}\end{bmatrix} \cdot P_n^m(\cos\theta)\begin{matrix}\cos\\ \sin\end{matrix}(m\phi) \tag{9a}$$

$$\begin{bmatrix} H_\theta^{>} \\ H_\theta^{<} \end{bmatrix} = \frac{ik_0^2}{4\pi}\sum_{n=1}^{\infty}\sum_{m=0}^{n} D_{mn}\left\{ \mp\begin{bmatrix} \boldsymbol{\Phi}^{N<}_{\substack{e\\o}mn}h_n^{(1)}(k_0r) \\ \boldsymbol{\Phi}^{N>}_{\substack{e\\o}mn}j_n(k_0r)\end{bmatrix} \cdot \frac{m}{\sin\theta}P_n^m(\cos\theta)\begin{matrix}\sin\\ \cos\end{matrix}(m\phi) + \frac{dP_n^m(\cos\theta)}{d\theta} \cdot \begin{matrix}\cos\\ \sin\end{matrix}(m\phi)\begin{bmatrix} \boldsymbol{\Phi}^{M<}_{\substack{e\\o}mn}\dfrac{d[rh_n^{(1)}(k_0r)]}{k_0rdr} \\ \boldsymbol{\Phi}^{M>}_{\substack{e\\o}mn}\dfrac{d[rj_n(k_0r)]}{k_0rdr}\end{bmatrix}\right\} \tag{9b}$$

$$\begin{bmatrix} H_\phi^{>} \\ H_\phi^{<} \end{bmatrix} = \frac{ik_0^2}{4\pi}\sum_{n=1}^{\infty}\sum_{m=0}^{n} D_{mn}\left\{ -\begin{bmatrix} \boldsymbol{\Phi}^{N<}_{\substack{e\\o}mn}h_n^{(1)}(k_0r) \\ \boldsymbol{\Phi}^{N>}_{\substack{e\\o}mn}j_n(k_0r)\end{bmatrix} \cdot \frac{dP_n^m(\cos\theta)}{d\theta}\begin{matrix}\cos\\ \sin\end{matrix}(m\phi) \mp \frac{m}{\sin\theta}P_n^m(\cos\theta) \cdot \begin{matrix}\sin\\ \cos\end{matrix}(m\phi)\begin{bmatrix} \boldsymbol{\Phi}^{M<}_{\substack{e\\o}mn}\dfrac{d[rh_n^{(1)}(k_0r)]}{k_0rdr} \\ \boldsymbol{\Phi}^{M>}_{\substack{e\\o}mn}\dfrac{d[rj_n(k_0r)]}{k_0rdr}\end{bmatrix}\right\}. \tag{9c}$$

From the above procedure, we can see that the derivation of the radiated fields is more general and straightforward than that given in [1]. Also, the closed form for a given current distribution is very compact, as seen from (5).

III. Fourier Series Current Distribution

Since any current distribution can be expanded into the Fourier series, to obtain the exact representation of the radiated fields, we assume that [1]

$$I(\phi') = \sum_{p=1}^{\infty} I_p \cos(p\phi'). \tag{10}$$

With this current distribution, the intermediates in (6) reduce to

$$\begin{bmatrix} \boldsymbol{\Phi}^{M<}_{emn} \\ \boldsymbol{\Phi}^{N>}_{emn} \end{bmatrix} = -\pi a(1+\delta_{m0})I_m\frac{dP_n^m(0)}{d\theta}\begin{bmatrix} j_n(k_0a) \\ h_n^{(1)}(k_0a)\end{bmatrix} \tag{11a}$$

$$\begin{bmatrix} \boldsymbol{\Phi}^{N<}_{omn} \\ \boldsymbol{\Phi}^{N>}_{omn} \end{bmatrix} = +m\pi a I_m P_n^m(0)\begin{bmatrix} \dfrac{d[aj_n(k_0a)]}{k_0ada} \\ \dfrac{d[ah_n^{(1)}(k_0a)]}{k_0ada}\end{bmatrix} \tag{11b}$$

since

$$\int_0^{2\pi}\begin{matrix}\cos\\ \sin\end{matrix}(m\phi')I(\phi') = \pi(1+\delta_{m0})I_m\begin{bmatrix}1\\0\end{bmatrix}.$$

It is noticed that the odd mode of $\boldsymbol{\Phi}^{M}_{\substack{e\\o}mn}$ and the even mode of $\boldsymbol{\Phi}^{N}_{\substack{e\\o}mn}$ in (6) vanish so that the radiated fields are further simplified to

$$\begin{bmatrix} \boldsymbol{E}^{>} \\ \boldsymbol{E}^{<} \end{bmatrix} = -\frac{\eta_0 k_0^2}{4\pi}\sum_{n=1}^{\infty}\sum_{m=0}^{n} D_{mn}\left\{\begin{bmatrix} \boldsymbol{\Phi}^{M<}_{emn}\boldsymbol{M}^{(1)}_{emn}(k_0) \\ \boldsymbol{\Phi}^{M>}_{emn}\boldsymbol{M}_{emn}(k_0)\end{bmatrix} + \begin{bmatrix} \boldsymbol{\Phi}^{N<}_{omn}\boldsymbol{N}^{(1)}_{omn}(k_0) \\ \boldsymbol{\Phi}^{N>}_{omn}\boldsymbol{N}_{omn}(k_0)\end{bmatrix}\right\} \tag{12a}$$

$$\begin{bmatrix}\boldsymbol{H}^{>}\\ \boldsymbol{H}^{<}\end{bmatrix} = \frac{ik_0^2}{4\pi}\sum_{n=1}^{\infty}\sum_{m=0}^{n} D_{mn}\left\{\begin{bmatrix}\boldsymbol{\Phi}_{emn}^{M<}\boldsymbol{N}_{emn}^{(1)}(k_0)\\ \boldsymbol{\Phi}_{emn}^{M>}\boldsymbol{N}_{emn}(k_0)\end{bmatrix} + \begin{bmatrix}\boldsymbol{\Phi}_{omn}^{N<}\boldsymbol{M}_{omn}^{(1)}(k_0)\\ \boldsymbol{\Phi}_{omn}^{N>}\boldsymbol{M}_{omn}(k_0)\end{bmatrix}\right\}. \quad (12b)$$

So far, the exact integration solution of the radiated fields has been evaluated analytically and presented in terms of the spherical Bessel functions and spherical harmonics. Numerical computation of the similar summation of the spherical Bessel and Hankel functions and the spherical harmonics in [25] and [26] shows that the summation converges rapidly and that at most 20 terms for the index n should be taken usually.

IV. Sinusoidal Current Distribution

As a degenerate form of the Fourier series form representation, the current distribution of the circular loop is commonly assumed to be a sinusoidal and varies along the circumference of the loop. Let $I_n = 0$ in the Fourier series expression except for $n \neq p$, we therefore have

$$I(\phi') = I_p \cos(p\phi'). \quad (13)$$

The solution of the radiated fields can be easily obtained by letting $I_m = I_p\delta_{mp}$ in (12). Substituting this relationship into (12), we obtain

$$\begin{bmatrix}\boldsymbol{E}^{>}\\ \boldsymbol{E}^{<}\end{bmatrix} = -\frac{\eta_0 k_0^2}{4\pi}\sum_{n=p}^{\infty} D_{pn}\left\{\begin{bmatrix}\boldsymbol{\Phi}_{epn}^{M<}\boldsymbol{M}_{epn}^{(1)}(k_0)\\ \boldsymbol{\Phi}_{epn}^{M>}\boldsymbol{M}_{epn}(k_0)\end{bmatrix} + \begin{bmatrix}\boldsymbol{\Phi}_{opn}^{N<}\boldsymbol{N}_{opn}^{(1)}(k_0)\\ \boldsymbol{\Phi}_{opn}^{N>}\boldsymbol{N}_{opn}(k_0)\end{bmatrix}\right\} \quad (14a)$$

$$\begin{bmatrix}\boldsymbol{H}^{>}\\ \boldsymbol{H}^{<}\end{bmatrix} = \frac{ik_0^2}{4\pi}\sum_{n=p}^{\infty} D_{pn}\left\{\begin{bmatrix}\boldsymbol{\Phi}_{epn}^{M<}\boldsymbol{N}_{epn}^{(1)}(k_0)\\ \boldsymbol{\Phi}_{epn}^{M>}\boldsymbol{N}_{epn}(k_0)\end{bmatrix} + \begin{bmatrix}\boldsymbol{\Phi}_{opn}^{N<}\boldsymbol{M}_{opn}^{(1)}(k_0)\\ \boldsymbol{\Phi}_{opn}^{N>}\boldsymbol{M}_{opn}(k_0)\end{bmatrix}\right\} \quad (14b)$$

where the intermediates $\Phi_{epn}^{M\lessgtr}$ and $\Phi_{opn}^{N\lessgtr}$ are given by (11) and the eigenvalue m is replaced by p. The components of the electromagnetic radiated fields can be easily obtained from the vector form in (14) by substituting the individual components of the vector-wave functions in (4), respectively, into (14).

V. Uniform Current Distribution

Uniform current distribution of the loop antenna, i.e., $I(\phi') = I_0$ where I_0 is a constant, represents the simplest case of the circular-loop antenna radiation. This assumption is valid and accurate enough for the circular-loop antennas which are electrically small in size. With this assumption, the exact solutions can be easily obtained, as dealt with in the past by Balanis [21], Stutzman and Thiele [19], Elliott [17], Kraus [20], and more recently by Werner [1] and Overfelt [2].

A. Exact Expressions in Terms of Spherical Harmonics

In fact, this case can be considered as a particularly special case of either the Fourier series, where only the first term exists; or the sinusoidal case, where the parameter $p = 0$. Therefore, we do not need to repeat the preceding derivation. Instead, we just specify the parameter $p = 0$ in the previously given formula (14). Substituting $m = 0$ into (11), we can see that both $\Phi_{o0n}^{N>}$ and $\Phi_{o0n}^{N<}$ are zero such that the electromagnetic fields in (14) are further simplified. Thus, we finally have the radiated fields expressed as

$$\begin{bmatrix}\boldsymbol{E}^{>}\\ \boldsymbol{E}^{<}\end{bmatrix} = -\frac{\eta_0 k_0^2}{4\pi}\sum_{n=0}^{\infty} D_{0n}\begin{bmatrix}\boldsymbol{\Phi}_{e0n}^{M<}\boldsymbol{M}_{e0n}^{(1)}(k_0)\\ \boldsymbol{\Phi}_{e0n}^{M>}\boldsymbol{M}_{e0n}(k_0)\end{bmatrix} \quad (15a)$$

$$\begin{bmatrix}\boldsymbol{H}^{>}\\ \boldsymbol{H}^{<}\end{bmatrix} = \frac{ik_0^2}{4\pi}\sum_{n=0}^{\infty} D_{0n}\begin{bmatrix}\boldsymbol{\Phi}_{e0n}^{M<}\boldsymbol{N}_{e0n}^{(1)}(k_0)\\ \boldsymbol{\Phi}_{e0n}^{M>}\boldsymbol{N}_{e0n}(k_0)\end{bmatrix} \quad (15b)$$

where, with the reduction $P_n^m(x)$ to $P_n(x)$ as $m = 0$

$$\begin{bmatrix}\boldsymbol{\Phi}_{e0n}^{M<}\\ \boldsymbol{\Phi}_{e0n}^{M>}\end{bmatrix} = -2\pi a I_0 \frac{dP_n(0)}{d\theta}\begin{bmatrix}j_n(k_0a)\\ h^{(1)}(k_0a)\end{bmatrix} \quad (16a)$$

$$D_{0n} = \frac{2n+1}{n(n+1)}. \quad (16b)$$

Since $m = 0$ in the vector-wave functions, the components of the radiated fields can be expressed by taking the scalar form of (15) as

$$\begin{bmatrix}E_r^{>}\\ E_r^{<}\end{bmatrix} = \begin{bmatrix}E_\theta^{>}\\ E_\theta^{<}\end{bmatrix} = 0 \quad (17a)$$

$$\begin{bmatrix}E_\phi^{>}\\ E_\phi^{<}\end{bmatrix} = \frac{\eta_0 k_0^2 a I_0}{2}\sum_{n=1}^{\infty}\frac{2n+1}{n(n+1)}\,\frac{dP_n(0)}{d\theta}\,\frac{dP_n(\cos\theta)}{d\theta} \cdot \begin{bmatrix}h_n^{(1)}(k_0r)j_n(k_0a)\\ j_n(k_0r)h_n^{(1)}(k_0a)\end{bmatrix} \quad (17b)$$

and

$$\begin{bmatrix}H_r^{>}\\ H_r^{<}\end{bmatrix} = -\frac{ik_0^2 a I_0}{2}\sum_{n=1}^{\infty}(2n-1)\frac{dP_n(0)}{d\theta}P_n(\cos\theta) \cdot \frac{1}{k_0r}\begin{bmatrix}h_n^{(1)}(k_0r)j_n(k_0a)\\ j_n(k_0r)h_n^{(1)}(k_0a)\end{bmatrix} \quad (18a)$$

$$\begin{bmatrix}H_\theta^{>}\\ H_\theta^{<}\end{bmatrix} = \frac{-ik_0^2 a I_0}{2}\sum_{n=1}^{\infty}\frac{2n+1}{n(n+1)}\,\frac{dP_n(0)}{d\theta}\,\frac{dP_n(\cos\theta)}{d\theta} \cdot \begin{bmatrix}\dfrac{d[rh_n^{(1)}(k_0r)]}{d_0r\,dr}j_n(k_0a)\\ \dfrac{d[rj_n(k_0r)]}{k_0r\,dr}h_n^{(1)}(k_0a)\end{bmatrix} \quad (18b)$$

$$\begin{bmatrix}H_\phi^{>}\\ H_\phi^{<}\end{bmatrix} = 0. \quad (18c)$$

It should be emphasized that (17) and (18) are the exact solutions of the electromagnetic radiated fields in the regions $r > a$ and $r < a$, respectively. Also it is noted that there is no any restriction on the dimension of loop antennas.

B. Simplified Components

Electrically Small Loop: For the electrically small loop (that is, $k_0a \ll 1$), we have [27]

$$j_n(k_0a) \approx \frac{2^n n!}{(2n+1)!}(k_0a)^n \quad (19a)$$

$$h_n^{(1)}(k_0a) \approx \frac{i}{2^n}\,\frac{(2n!}{n!}\,\frac{1}{(k_0a)^{n+1}}. \quad (19b)$$

Therefore, the solution for this case can be found instantly from the general solutions in (17) and (18) by taking the first term of the summation (i.e., assuming $n = 1$ only)

$$\begin{bmatrix} E_\phi^> \\ E_\phi^< \end{bmatrix} = -\frac{\eta_0 k_0^3 a^2 I_0}{4} \sin\theta \begin{bmatrix} h_1^{(1)}(k_0 r) \\ \frac{3i}{(k_0 a)^3} j_1(k_0 r) \end{bmatrix} \tag{20a}$$

$$\begin{bmatrix} H_r^> \\ H_r^< \end{bmatrix} = \frac{i(k_0 a)^2 I_0}{2r} \cos\theta \begin{bmatrix} h_1^{(1)}(k_0 r) \\ \frac{3i}{(k_0 a)^3} j_1(k_0 r) \end{bmatrix} \tag{20b}$$

$$\begin{bmatrix} H_\theta^> \\ H_\theta^< \end{bmatrix} = -\frac{i k_0^3 a^2 I_0}{4} \sin\theta \begin{bmatrix} \frac{d[r h_1^{(1)}(k_0 r)]}{k_0 r dr} \\ \frac{3i}{(k_0 a)^3} \frac{d[r j_1(k_0 r)]}{k_0 r dr} \end{bmatrix} \tag{20c}$$

since

$$P_1(\cos\theta) = \cos\theta, \quad \text{and} \quad \frac{dP_1(\cos\theta)}{d\theta} = -\sin\theta.$$

To confirm the correctness of the above formulation, we make use of the following formula [28]:

$$h_n^{(1)}(k_0 r) = (-i)^{n+1} \frac{e^{ik_0 r}}{k_0 r} \sum_{\ell=0}^{n} i^\ell \frac{(n+\ell)!}{\ell!(n-\ell)!} \left(\frac{1}{2k_0 r}\right)^\ell \tag{21a}$$

so that

$$\frac{1}{k_0 r} \frac{d[r h_n^{(1)}(k_0 r)]}{dr} = (-i)^{n+1} \frac{e^{ik_0 r}}{k_0 r} \sum_{\ell=0}^{n} i^\ell \frac{(n+\ell)!}{\ell!(n-\ell)!} \cdot \left(i - \frac{\ell}{k_0 r}\right) \left(\frac{1}{2k_0 r}\right)^\ell. \tag{21b}$$

By taking only the first two terms for $n = 1$, these two functions reduce to the following forms:

$$h_1^{(1)}(k_0 r) = -\frac{e^{ik_0 r}}{k_0 r} \left(1 - \frac{1}{ik_0 r}\right) \tag{22a}$$

$$\frac{1}{k_0 r} \frac{d[r h_1^{(1)}(k_0 r)]}{dr} = -i \frac{e^{ik_0 r}}{k_0 r} \left[1 - \frac{1}{ik_0 r} - \left(\frac{1}{k_0 r}\right)^2\right]. \tag{22b}$$

With the substitution of (22) into (20), the general formulas in (17) and (18) reduce to the following well-known results:

$$E_\phi^> = \frac{\eta_0 (k_0 a)^2 I_0}{4r} \sin\theta e^{ik_0 r} \left(1 - \frac{1}{ik_0 r}\right) \tag{23a}$$

$$H_r^> = -\frac{i(k_0 a)^2 I_0}{2k_0 r^2} \cos\theta e^{ik_0 r} \left(1 - \frac{1}{ik_0 r}\right) \tag{23b}$$

$$H_\theta^> = -\frac{(k_0 a)^2 I_0}{4r} \sin\theta e^{ik_0 r} \left[1 - \frac{1}{ik_0 r} - \left(\frac{1}{k_0 r}\right)^2\right] \tag{23c}$$

except that the sign of the imaginary symbol i is changed due to the different time dependence chosen.

As shown in the form given previously in (20), the results given in (23) are valid *only* in the outer spherical region where $r > a$. The radiated fields in the inner spherical region where $r < a$ are given by the fields $\boldsymbol{E}^<$ and $\boldsymbol{H}^<$ in (20). However, this validity was *not realized* in the past, as stated by Banalis [21, p. 169] that "the fields radiated by a small loop, as given by (5-18a)–(5-19b) [in fact, (23a) and (23b)] are valid everywhere except at the origin."

C. Simplified Components

Far-Zone Fields: To obtain the far-zone results, we may make use of the following approaches (see [23, p. 217] or [27]):

$$h_n^{(1)}(k_0 r) \approx (-i)^{n+1} \frac{e^{ik_0 r}}{k_0 r} \tag{24a}$$

$$\frac{1}{k_0 r} \frac{d[r h_n^{(1)}(k_0 r)]}{dr} \approx (-i)^n \frac{e^{ik_0 r}}{k_0 r}. \tag{24b}$$

Also, the following recurrence relations are needed for further reduction [23, p. 205]:

$$\frac{dP_n^m(\cos\theta)}{d\theta} = \frac{1}{2}[(n-m+1)(n+1)P_n^{m-1} - P_n^{m+1}] \tag{25a}$$

$$m \cot\theta P_n^m(\cos\theta) = \frac{1}{2}[(n-m+1)(n+1)P_n^{m-1} + P_n^{m+1}]. \tag{25b}$$

Furthermore, we have by letting $m = 0$ in (25) and thereafter canceling the term $n(n+1)P_n^{-1}$

$$\frac{dP_n(\cos\theta)}{d\theta} = -P_n^1(\cos\theta). \tag{26}$$

By substituting (26) and (24) into the general form of the radiated fields in (17) and (18), we have

$$E_r^> = E_\theta^> = 0 \tag{27a}$$

$$E_\phi^> \approx \frac{\eta_0 k_0 a I_0}{2} \frac{e^{ik_0 r}}{r} \sum_{n=1}^{\infty} (-i)^{n-1} \frac{2n+1}{n(n+1)} \cdot P_n^1(0) P_n^1(\cos\theta) j_n(k_0 a) \tag{27b}$$

$$H_r^> \approx H_\phi^> = 0 \tag{27c}$$

$$H_\theta^> \approx -\frac{k_0 a I_0}{2} \frac{e^{ik_0 r}}{r} \sum_{n=1}^{\infty} (-i)^{n-1} \frac{2n+1}{n(n+1)} \cdot P_n^1(0) P_n^1(\cos\theta) j_n(k_0 a). \tag{27d}$$

It is given by Flammer [29] (for one form with plus sign) and by Li *et al.* [30] (for the other form with minus sign) that

$$J_m(kr\sin\theta) = \sum_{n=0}^{\infty} (\pm i)^{n-m} (2n+1) \frac{(n-m)!}{(n+m)!} \cdot P_n^m(0) P_n^m(\cos\theta) j_n(kr). \tag{28}$$

Therefore, (17)–(27) again reduce to the well-known components form of the far-zone electric and magnetic fields as follows:

$$E_r^> = E_\theta^> = 0 \tag{29a}$$

$$E_\phi^> \approx \frac{\eta_0 k_0 a I_0}{2} \frac{e^{ik_0 r}}{r} J_1(k_0 a \sin\theta) \tag{29b}$$

$$H_r^> \approx H_\phi^> = 0 \tag{29c}$$

$$H_\theta^> \approx -\frac{k_0 a I_0}{2} \frac{e^{ik_0 r}}{r} J_1(k_0 a \sin\theta) \tag{29d}$$

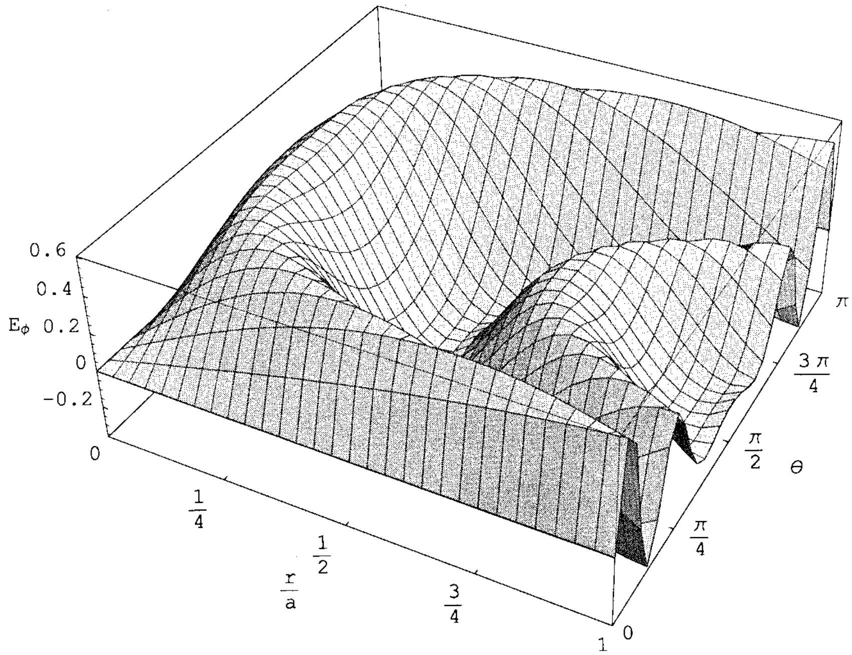

(a)

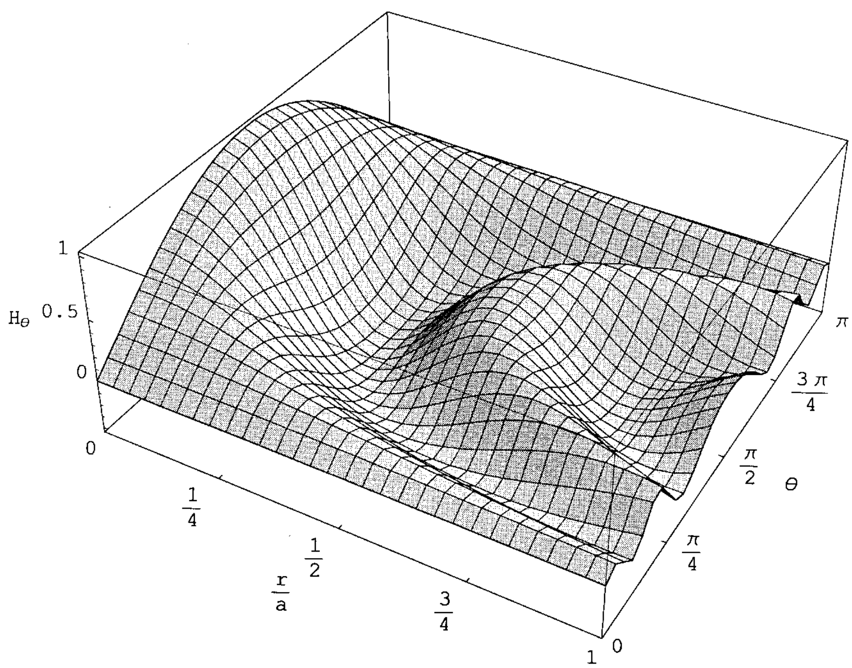

(b)

Fig. 2. Three-dimensional normalized patterns of near zone E_ϕ-component and H_θ-component as a function of θ for various values of r. (a) E_ϕ field pattern. (b) H_θ field pattern.

which were given by Balanis [21] and again obtained from the far-zone approximation by Werner [1]. Instead of $e^{i\omega t}$ in either [21] or [1], the paper assumes the time dependence $e^{-i\omega t}$ so that again the forms presented here take the conjugate forms of [21] and [1].

VI. Numerical Results

As stated, the radiated fields $\boldsymbol{E}^{>}$ and $\boldsymbol{H}^{>}$ in the near and far zones in the spherical outer region $r > a$ radiated due to the loop antenna carrying a uniform current are given by (20). Error analysis of the approximate results such as those in (23) for an electrically small loop and in (29) for the far-field approxmiation have already been carried out numerically by Werner [1] and Overfelt [2] based on the exact series expression. Therefore, this paper will not repeat it. However, the near fields $\boldsymbol{E}^{<}$ and $\boldsymbol{H}^{<}$ in the spherical inner region $r < a$ radiated due to the uniform current loop given by (20) were not reported elsewhere. Also, they were sometimes mistaken to be $\boldsymbol{E}^{>}$ and $\boldsymbol{H}^{>}$ in (23). To gain an insight into these near fields, this paper will present the antenna E-plane and H-plane

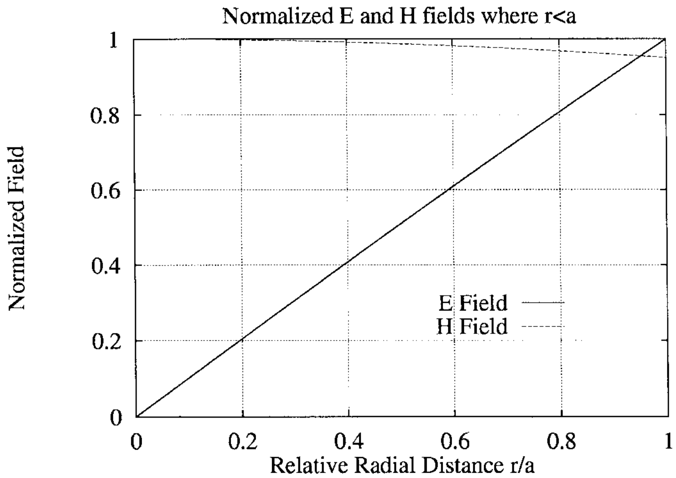

Fig. 3. Normalized electric (E_ϕ component with respect to $r = a$) and magnetic (H_θ component with respect to $r = 0$) fields inside the spherical region $r < a$ against the radial distance r.

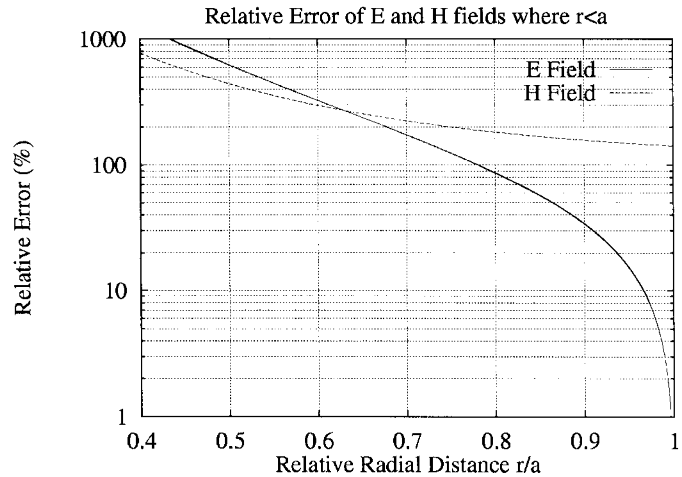

Fig. 4. Relative error of the electric (E_ϕ component) and magnetic (H_θ component) fields inside the spherical region $r < a$.

patterns based on the exact results in (20), together with an error analysis.

Consider a circular loop of radius $a = 2\lambda$. If the loop dimension is very small, the antenna pattern is, as can be seen from (20), just a sinusoidal or cosine pattern. However, when the loop size becomes larger, e.g., $ka = 4\pi \gg 1$, it is no longer this type of patterns. Under this approximation, the field components E_ϕ and H_θ are approximated as

$$E_\phi^< \approx \frac{\eta_0 k_0 I_0}{2} e^{ik_0 a} J_1(k_0 r \sin\theta) \tag{30a}$$

$$H_\theta^< \approx i\frac{k_0 I_0}{2} e^{ik_0 a} \sin\theta J_0(k_0 r \sin\theta) \tag{30b}$$

since

$$\left(\frac{d}{xdx}\right)^m [x^n J_n(x)] = x^{n-m} J_{n-m}(x)$$

where $m = 1$ and $n = 1$ are assumed.

Its near-field patterns of $J_1(kr\sin\theta)$ and $\sin\theta J_0(kr\sin\theta)$ in (30) due to such a loop of radius $a = 2\lambda$ are normalized and plotted in Fig. 2. It is seen that the antenna pattern varies with the radial distance for $r \leq a$. Due to the symmetry of the pattern, only the range $(0 \rightarrow \pi)$ for the spherical polar angle θ is considered. At the center of the loop, both patterns are of the sine functional shape. When the observation point is quite close to the loop, both the E-plane and H-plane patterns of the loop become complicated.

Both the electric (E_ϕ component) and magnetic (H_θ component) fields in the inner spherical region $r < a$ are computed numerically and shown in Fig. 3 as a function of the radial distance by using (20). The electric field is normalized to the field value at $r = a$ and the magnetic field to that at $r = 0$. It is seen that the electric field is zero at the origin while the magnetic field is at the maximum in the inner region. This is physically true, as can be confirmed by the *Biot–Savart law*. From this variation, it is definitely sure that (23) cannot be used to represent the fields inside the sphere $r = a$ since both electric and magnetic fields in (23) approach infinity as $r \rightarrow 0$.

To show the difference between the actual fields in (20) and the assumed near fields in (23), Fig. 4 depicts the variation of the relative error of both electric and magnetic field components E_ϕ and H_θ in the region where $r < a$. In the computation, the angle $\theta = \pi/2$ is assumed since this plane is of particular interest. It is seen that the error of the E_ϕ component increases tremendously at an observation point near the loop although the continuity of the component exists where the error is zero. At $r = a, 0.9a, 0.8a, 0.7a, 0.6a,$ and $0.5a$, the relative error of E_ϕ is about 0, 34, 86, 161, 325, and 624%. The relative error of the magnetic field component H_θ varies with r slowly compared to the electric field. At $r = a, 0.9a, 0.8a, 0.7a, 0.6a,$ and $0.5a$, the relative error of H_θ is about 141, 157, 181, 223, 296, and 442%. When $H_\theta^>$ is used to represent $H_\theta^<$ inside the region $r < a$, however, a very large error is present everywhere. At a point around origin, the relative errors of both E_ϕ and H_θ approach infinity. It should be pointed out that the first term of (17) is used to calculate the error since it is more accurate than the approximated formulas (20).

VII. Conclusions

This paper presents an alternative method for obtaining electromagnetic radiated fields due to circular-loop antennas of arbitrary radius. The method is more general, compact and straightforward, as compared with the recent two methods published. In particular, the results are valid for the regions of both $r > a$ and $r < a$. With this method, the closed-form solution of radiated fields due to circular loops which carry the current distribution $I(\phi')$ can be obtained as long as the function $I(\phi')\genfrac{}{}{0pt}{}{\cos}{\sin}(m\phi')$ is integratable analytically. To show how the exact results are obtained, a general current distribution that is expanded into the Fourier cosine series is considered. Then, two applications are made where the exact fields everywhere due to a sinusoidal and a uniform loop current distributions are derived. Finally, the method is confirmed by applying it to obtain the exact results for the uniform current distribution, and the well-known approximate results by asymptotic expansions (i.e., the far fields due to loops of any dimension and the radiated fields due to electrically small loops). Numerical error analysis is carried out and antenna patterns of the near fields where $r < a$ are plotted and discussed.

REFERENCES

[1] D. H. Werner, "An exact integration procedure for vector potentials of thin circular loop antennas," *IEEE Trans. Antennas Propagat.*, vol. 44, pp. 157–165, Feb. 1996.

[2] P. L. Overfelt, "Near fields of the constant current thin circular loop antenna of arbitrary radius," *IEEE Trans. Antennas Propagat.*, vol. 44, pp. 166–171, Feb. 1996.

[3] D. Foster, "Loop antennas with uniform current," *Proc. IRE*, vol. 32, pp. 603–607, Oct. 1944.

[4] J. B. Sherman, "Circular loop antennas with uniform current," *Proc. IRE*, vol. 32, pp. 534–537, Sept. 1944.

[5] G. Glinski, "Note on the circular loop antennas with nonuniform current distribution," *J. Appl. Phys.*, vol. 18, pp. 638–644, July 1947.

[6] J. E. Lindsay, Jr., "A circular loop antenna with nonuniform current distribution," *IRE Trans. Antennas Propagat.*, vol. AP-8, pp. 439–441, July 1960.

[7] E. J. Martin, Jr., "Radiation fields of circular loop antennas by a direct integration process," *IRE Trans. Antennas Propagat.*, vol. AP-8, pp. 105–107, Jan. 1960.

[8] T. T. Wu, "Theory of the thin circular loop antenna," *J. Math. Phys.*, vol. 3, pp. 1301–1304, 1962.

[9] F. M. Greene, "The near-zone magnetic field of a small circular-loop antenna," *J. Res. NSB*, vol. 71-C, no. 4, pp. 319–326, Oct. 1967.

[10] B. R. Rao, "Far-field patterns of large circular loop antennas: Theoretical and experimental results," *IEEE Trans. Antennas Propagat.*, vol. AP-16, pp. 269–270, Mar. 1968.

[11] S. M. Prasad and B. N. Das, "A circular loop antenna with traveling wave current distribution," *IEEE Trans. Antennas Propagat.*, vol. AP-18, pp. 278–280, Mar. 1970.

[12] G. S. Smith, "Loop antennas," in *Antenna Engineering Handbook*. New York: McGraw-Hill, 1984.

[13] J. R. Wait, "Insulated loop antenna immersed in a conducting medium," *J. Res. NBS*, vol. 59, no. 2, pp. 133–137, Aug. 1957.

[14] ——, "A note on the insulated loop antenna immersed in a conducting medium," *Radio Sci. J. Res. NBS*, vol. 68-D, no. 11, pp. 1249–1250, Nov. 1964.

[15] R. H. Williams, "Insulated and loaded loop antenna immersed in a conducting medium," *Radio Sci. J. Res. NBS*, vol. 69-D, no. 2, pp. 287–289, Feb. 1965.

[16] S. A. Schelkunoff, *Advanced Antenna Theory*. New York: Wiley, 1952.

[17] R. S. Elliott, *Antenna Theory and Design*. Englewood Cliffs, NJ: Prentice-Hall, 1981.

[18] R. W. P. King and G. S. Smith, *Antennas in Matter: Fundamentals, Theory and Applications*. Cambridge, MA: MIT Press, 1981.

[19] W. L. Stutzman and G. A. Thiele, *Antenna Theory and Design*. New York: Wiley, 1981.

[20] J. D. Kraus, *Antennas*, 2nd ed. New York: McGraw-Hill, 1981.

[21] C. A. Balanis, *Antenna Theory: Analysis and Design*. New York: Wiley, 1982.

[22] R. E. Collin, *Antennas and Radiowave Propagation*. New York: McGraw-Hill, 1985.

[23] C. T. Tai, *Dyadic Green's Functions in Electromagnetic Theory*, 2nd ed. Piscataway, NJ: IEEE Press, 1994.

[24] L. W. Li, P. S. Kooi, M. S. Leong, and T. S. Yeo, "Electromagnetic dyadic Green's function in spherically multilayered media," *IEEE Trans. Microwave Theory Tech.*, vol. 42, pt. A, pp. 2302–2310, Dec. 1994.

[25] L. W. Li, P. S. Kooi, M. S. Leong, T. S. Yeo, and X. Ma, "An analysis of a circular aperture antenna covered with a dielectric hemispherical shell radome over ground plane," in *Dig. IEEE AP-S Int. Symp. USNC/URSI Radio Sci. Meet.*, Newport Beach, CA, vol. 3, June 1995, pp. 1442–1445.

[26] M. S. Leong, L. W. Li, P. S. Kooi, T. S. Yeo, and X. Ma, "Layered hemispherical radome analysis including effects of rainfall," in *Proc. Malaysia Int. Conf. Commun. (MICC'95)*, Langkawi Island, Malaysia, Nov. 1995, pp. 12.3.1–12.3.4.

[27] J. A. Stratton, *Electromagnetic Theory*. New York: McGraw-Hill, 1941.

[28] I. S. Gradshteyn and I. M. Ryzhik, *Tables of Integrals, Series, and Products*. New York: Academic, 1980.

[29] C. Flammer, *Spheroidal Wave Functions.* Stanford, CA: Stanford Univ. Press, 1957.

[30] L. W. Li, T. S. Yeo, P. S. Kooi, M. S. Leong, and X. Ma, "Full-wave analysis of a circular aperture antenna covered with a dielectric hemispherical shell radome over ground plane," *IEEE Trans. Antennas Propagat.*, to be published.

Le-Wei Li (S'91–M'92–SM'96) received the B.Sc. degree in physicsfrom Xuzhou Normal University, Xuzhou, China, in 1984, the M.Eng.Sc. degree in electrical engineering from the China Research Institute of Radiowave Propagation (CRIRP), Xinxiang, China, in 1987, and the Ph.D. degree from Monash University, Melbourne, Australia, in 1992.

From 1987 to 1989, he spent two years in Ionospheric Propagation Laboratory at the CRIRP, Xinxiang, China. In 1992 he worked at La Trobe University (jointly with Monash University), Melbourne, Australia, as a Research Fellow. Since 1992 he has been with the Department of Electrical Engineering, National University of Singapore, where he is currently a Senior Lecturer. His current research interests include electromagnetic theory, radio wave propagation and scattering in various media, microwave propagation and scattering in tropical environment, and antenna radiation.

Mook-Seng Leong (M'81) received the B.Sc. (electrical engineering with first class honors) and Ph.D. degrees (microwave engineering) from the University of London, U.K., in 1968 and 1971, respectively.

He is currently a Professor of electrical engineering at the National University of Singapore. He is a member of the Editorial Board for *Microwave and Optical Technology Letters*. His main research interests include antenna and waveguide boundary-value problems and semiconductor characterization using the SRP technique.

Dr. Leong is a member of the MIT-based Electromagnetic Academy and a Fellow of the Institute of Electrical Engineers, London, U.K. He received the 1996 Defence Science Organization (DSO) Research and Development Award from DSO National Laboratories, Singapore, in 1996.

Pang-Shyan Kooi (M'75) received the B.Sc. degree in electrical engineering from the National Taiwan University, Taipei, in 1961, the M.Sc. degree in electrical engineering from UMIST, Manchester, U.K., in 1963, and the D.Phil. degree in engineering science from Oxford University, U.K., in 1970.

Since 1970, he has been with the Electrical Engineering Department of the National University of Singapore, where he is currently a Professor of electrical enginnering. His current research interests are microwave and millimeter-wave circuits and antennas.

Tat-Soon Yeo (M'80–SM'93) received the B.Eng. (honors) and M.Eng. degrees from the National University of Singapore in 1979 and 1981, respectively, and the Ph.D. degree from the University of Canterbury, New Zealand, in 1985.

Since 1985, he has been with the Electrical Engineering Department, National University of Singapore, where he is currently an Associate Professor. His current research interests are in wave propagation and scattering, antennas, and numerical techniques.

Dr. Yeo received the 1997 Defence Science Organization (DSO) Research and Development Award from DSO National Laboratories, Singapore, in 1997. He is also the Chairman of the MTT/AP/EMC joint Chapter, Singapore IEEE Section.